AIChE WILEY InterScience DISCOVER SOMETHING GREAT

Controlling Fine Particle Formation Processes using a Concentric Microreactor

Hideharu Nagasawa
Frontier Core Technology Laboratories, FUJIFILM Corporation, 577, Ushijima, Kaisei-machi, Ashigarakami-gun, Kanagawa 258-8577, Japan, and Dept. of Chemical Engineering, Kyoto University, Kyoto-daigaku Katsura, Nishikyo-ku, Kyoto 615-8510, Japan

Tatsuya Tsujiuchi, Taisuke Maki, and Kazuhiro Mae
Dept. of Chemical Engineering, Kyoto University, Kyoto-daigaku Katsura, Nishikyo-ku, Kyoto 615-8510, Japan

DOI 10.1002/aic.11049
Published online November 30, 2006 in Wiley InterScience (www.interscience.wiley.com).

To clarify the mechanism of fine-particle formation processes in a multilamination type microreactor that proceeds mainly due to molecular-diffusion-induced mixing, the relation between the size and distribution, and reaction-operation condition in experimental and numerical approaches is investigated. For experimental study, a concentric microreactor was used, and titania fine-particle formation was examined as a model reaction. Based on the hypothesis on the fine-particle formation mechanism, from the experimental results derived, a relatively simple calculation model was made, and validity demonstrated by showing the coincidence of the calculation results and the experimental results. Also, the calculation model was used to establish a technique for predicting the reactant concentration profiles in the microchannel, particle-growth rate, number of formed particles, and nucleation region. Thus, the proposed analysis method will be useful as a guideline for designing microreactors to form fine particles, and will provide industrially information. © 2006 American Institute of Chemical Engineers *AIChE J,* 53: 196–206, 2007
Keywords: microreactor, annular multilamination, particle-formation process, fine particles, titania

Introduction

Particles are now widely used for materials of various kinds of chemical industry products, such as electronic display, color inks and medical supplies. The performance of these products is strongly affected by particle properties, such as the particle sizes, the distribution of the sizes and the shapes. In recent years, fine particles, which diameters are 1μm or less, and monodispersed particles have been developed to advance their functionalities and add value to chemical industry products. In particular, monodispersed ultrafine particles, which diameters are 100 nm or less, are highly required. For example, the drug delivery system (DDS) of cancer treatment requires monodispersed carrier particles of the size 10 – 100 nm for selective dosing against cancer cells, based on the enhanced permeability and retention effect (EPR Effect).[1] The precise control of the particle properties, is, therefore, an extremely important technology for industrial use.

Method of fine-particle formation can be classified into two categories. One is a breakdown method, a physical method that mills law materials mechanically. Another is a buildup method, a chemical method that utilizes chemical reactions or crystallization of the gas or liquid phase. The breakdown method is widely used for actual fine-particle production, but needs a significantly large amount of power and long processing time, which is expensive. In contrast, the buildup method, in particular that of the liq-

Correspondence concerning this article should be addressed to K. Mae at kaz@cheme.kyoto-u.ac.jp.

© 2006 American Institute of Chemical Engineers

uid phase is appropriate time, as a fine-particle-formation method because of reaction controllability and productivity.

The mechanism of particle formation with the buildup method has long been studied. LaMer et al. proposed the so-called LaMer diagram, a conceptual diagram to present the particle-forming process, and explained the nucleation process, and the particle-growth process emphasizing the relation among the precursor concentration, the solubility product and the minimum critical supersaturation.[2] The idea became the basis for studying particle formation, and has been incorporated in many researches. In some cases, particle growth in the aggregation process and in other cases precipitation occurs on the surface of nuclei as in Ostwald ripening. The particle-growth mechanism has been studied in detail with several models.[3–6]

In actual particle production, the interrelation between the chemical reaction behaviors related to particle forming, and the physical behaviors, such as mixing condition at the field of particle formation is an essential factor for determining the particle properties. High-precision mixing control is required in order to realize desired particle properties of fine particles, such as narrow-size distribution. Various types of reactors have been developed for forming fine particles. For example, microreactors accurately control mixing and the reaction, and, hence, can be used for controlling particle properties, and many researchers on fine-particle formation have been performed with microreactors in recent years.[7–13] For example, Schenk et al.[7] developed two types of the separation layer mixer, named concentric and stacked separation layer micromixer, and presented a new concept for antifouling microchemical processing with solids precipitation from experimental and numerical approaches. There are two types of mixing in microreactors: convection mixing and precise mixing via interface by controlled-molecular diffusion.[14] Experimental and numerical researches have been performed on fine particle formation in convection mixing. Nagasawa et al. developed a new microreactor that utilizes microsegments collision for convection mixing. The authors conducted experiments on polystyrene fine particles, and showed that the reactor was useful for forming fine particles with narrow distribution.[15] Schwarzer et al. investigated the relation between the mixing and the particle size and distribution in fine particles formation.[16–19] They conducted fine particles formation of barium sulfate utilizing a microreactor with T-shaped channel, and estimated the particle size and distribution of the fine particles by a direct-numerical simulation (DNS) method, based on the population-balance equation. They showed that the simulation results coincided well with the experimental results.[19] On the other hand, there have been several researches on fine-particle formation in precise mixing via interface by controlled molecular diffusion. Wille et al. used the multilamination type microreactor developed by CPC-Systems to form ultrafine pigment particles of a mean-particle size of 90 nm, and showed that the particles are smaller in size than those formed by the conventional batch method.[20] Takagi et al. developed a concentric microreactor of clogging-free structure in the microchannel to form titania fine particles, and showed that the reactor could form the spherical fine particles with narrow-size distribution.[21]

Thus, it was shown that microreactors are effective for forming fine particles with narrow-size distribution. It was also shown that the particle size and distribution could be numerically estimated in the convection mixing type microreactors by the DNS method which generally needed much calculation loads. However, in the precise mixing via interface by controlled-molecular diffusion, the relation between the particle formation, and the physical behavior, such as mixing condition at the field of particle formation is not clear and no research has been performed on the estimation of particle size and distribution. For this reason, the size-control technology for forming fine particles with narrow-size distribution of the desired particle size and guidelines for the design of a detailed structure, and configuration of microreactors has not been established. In this study, we clarify the mechanism of particle formation process in the multilamination type microreactor that utilizes precise mixing via interface by controlled-molecular diffusion, and analyze methods of estimating the particle-number distribution in the nucleation and particle-growth processes.

Experimental

Reaction scheme for fine-particle formation

In this study, we conducted titania fine particle formation as a model reaction of fine-particle formation from liquid phases with the buildup method. The reaction formulas are given in Eqs. 1 and 2

$$\mathrm{Ti(OC_3H_7)_4 + 4H_2O \rightarrow Ti(OH)_4 + 4C_3H_7OH} \quad (1)$$

$$\mathrm{Ti(OH)_4 \rightarrow TiO_2 \cdot \mathit{x}H_2O + (1-\mathit{x}) \cdot H_2O} \quad (2)$$

This reaction by the alkoxide hydrolysis has an advantage in industrial productivity since the reaction is fast at room-temperature forming high-purity fine metal particles. However, the high-reaction rate makes it difficult to control, that is, high-precipitation rate and small solubility product.

In this experiment, we used the following reactant solutions: 1-octanol solution (Reactant A) of titanium tetraiso propoxide (TTIP: $Ti(OC_3H_7)_4$) and isopropanol solution (Reactant B) of water.

Experimental setup and reactors

Figure 1 shows the overview of the experimental setup. A 50 mL glass syringe, and a 60 mL of plastic syringe were filled, respectively, with the two reaction solutions, Reactant A and Reactant B, which were sent to a microreactor by microfeeder (KD Scientific; IC-3210).

Figure 2 presents the microreactor of concentric that we used in the experiment. The microreactor consists of a transparent glass pipe (external pipe) of inner dia. ($ID_{\mathrm{Layer\ B}}$) 1,500 μm, and a stainless pipe (internal pipe) of outer dia. ($OD_{\mathrm{Layer\ A}}$) 460 μm and inner dia. ($ID_{\mathrm{Layer\ A}}$) 320 μm. The pipes are placed coaxially, forming a dual pipe structure. The dual pipe structure connects to a microreaction channel of length (L) 191 mm, that is formed by the external pipe. A thermo jacket surrounds the external pipe for temperature control. Reactant solution is introduced in each of the inner and outer pipe areas in the dual-pipe structure of the microreactor. In the microreaction channel, two stratified flows are generated and fine particles are formed in the interface between the two reactant solutions. The flow generated in the inner pipe is called Layer A, and that generated in the outer pipe is called Layer B. This reaction operation method has

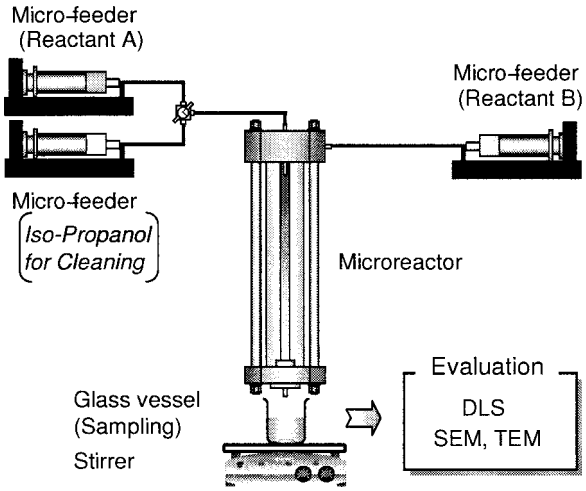

Figure 1. Experimental setup.

a distinguished feature: The diameter of the inner laminar flow of the annular currents can be controlled by changing the volume flow rate of the inner and outer reactant solutions, without changing the structure of the microreactor, and that the temperature gradient and concentration gradient in the interface between the two solutions can be controlled by changing the temperature and concentration of the outer layer solution. Another feature is that the interface between the two reactant solutions in the microreaction channel does not touch the pipe walls, and, hence, technical problems, such as clogging do not arise since formed fine particles do not adhere to the wall.

To show the technical superiority of the fine-particle formation technique with the microreactor, we also conducted an experiment by using a conventional method with a typical-batch reactor for comparison.

Experimental conditions

The nucleation and particle growth of titania fine particles vary with the relation among the reactant concentrations in the reaction field, minimum critical supersaturation, and solubility. In the multilamination type microreactor that utilizes a molecular-diffusion-induced mixing process, the reactant concentration in the reaction field changes dynamically in the flow direction z [m], and the radial direction r [m] of the annular pipe's microchannel perpendicular to the flow direction, since the molecules diffuse as they flow in the microchannel. Therefore, in consideration of Fick's law, the molecular diffusion time of reactants, and the concentration gradient are important factors in clarifying the mechanism of the dynamic fine-particle formation process.

According to the earlier view, to investigate the relation between the reaction control condition and the size and distribution of formed titania fine particles, we used the following parameters in the concentric microreactor experiment: (a) mean-residence time $T_{\text{Ave.}}$ [s], (b) TTIP concentration C_{TTIP} [vol. %] of the TTIP-1-octanol solution (Reactant A), and (c) water concentration C_{Water} [vol. %] of the water-isopropanol solution (Reactant B). The common experimental conditions set as follows: (1) TTIP-1-octanol solution (Reactant A), and water-isopropanol solution (Reactant B) were put, respectively, in Layers A and B, (2) the volume-flow rate of Reactant A, Q_A [mL/min], and of Reactant B, Q_B [mL/min], were set to make the ratio of the mean-linear velocities V_A [m/s] and V_B [m/s], that is, V_{Ratio} ($= V_A/V_B$), constant, and (3) the reaction temperature *Temp*. [K] was set to room-temperature (about 298 K).

Table 1 shows the experimental condition of each parameter. In the experiment (Table 1a) on the effect of the mean-residence time $T_{\text{Ave.}}$ in the microreactor, we changed $T_{\text{Ave.}}$ in the range from 0.7 to 4.5 s by changing Q_A and Q_B with V_{Ratio} being kept constant. With these parameters, the mean-linear velocity $V_{\text{Ave.}}$ in the microreaction channel was 0.04–0.26 m/s, and Reynolds number *Re*, which was calculated by $V_{\text{Ave.}} ID_{\text{Layer B}}/v_{\text{Ave.}}$, where $v_{Ave.}$ was the coefficient of kinematic viscosity of the mixed solution ($= 4 \times 10^{-5}$ m^2/s) was smaller than 96. This indicates that a laminar flow state was well formed, and a stable reaction interface was created, which was confirmed in visualization experiments. In the experiment, the TTIP concentration C_{TTIP} of Reactant A and the water concentration C_{Water} of Reactant B, were set as $C_{\text{TTIP}} = 1.0$ vol. % and $C_{\text{Water}} = 34.0$ vol. %. In the experiment (Table 1b) on the effect of the TTIP concentration C_{TTIP} of Reactant A, we chose $Q_A = 3.40$ mL/min, $Q_B = 23.71$ mL/min, and $C_{\text{Water}} = 34.0$ vol. %, and changed C_{TTIP} in the range from 1.0 to 9.0 vol. %. In the experiment (Table 1c) on the water concentration C_{Water} of Reactant B, we chose $Q_A = 3.40$ mL/min, $Q_B = 23.71$ mL/min, and $C_{\text{TTIP}} = 1.0$ vol. %, and changed C_{Water} in the range from 10.0 to 50.0 vol. %.

In the comparative experiment with the batch reactor, we put 23.71 mL of 34.0 vol. % water-isopropanol solution (Reactant B), and a stirrer in a 30-mL sample vessel at room-temperature (about 298 K). While stirring the solution at a rotation speed 500 rpm, 3.40 mL of 1.0 vol. % Reactant A were quickly added to Reactant B with a pipette. The solution-adding time was appropriately controlled to compare with the result ($T_{\text{Ave.}} =$ 0.7 s) of the experimental condition Ta-1 in the concentric microreactor.

The fine particle samples produced were served to a dynamic light scattering nanoparticle size analyzer (LB-550, HORIBA, Ltd.: DLS) to measure the mean size and distribution of the formed titania fine particle samples, and served to a scanning electron microscope (JEOL, Ltd.: SEM), and a transmission electron microscope (JEOL, Ltd.: TEM) to make qualitative

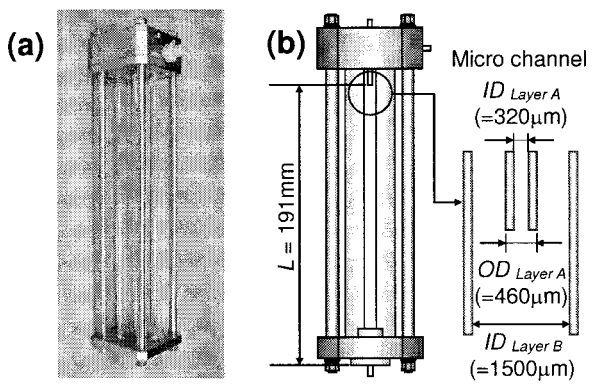

Figure 2. The microreactor: (a) the overview, and (b) the dimensions.

Table 1. Experimental Conditions for the Formation of Titania Fine particles Using the Concentric Microreactor

(a) Average Residence Time[a]

Test No.	Flow Rate [mL/min] Q_A	Q_B	Ave. Velocity [m/s] V_A	V_B	$V_{Ave.}$	Reynolds Number [−] Re	Ave-Residence Time [s] $T_{Ave.}$
Ta-1	3.40	23.71	0.71	0.25	0.26	95.9	0.7
Ta-2	1.70	11.86	0.35	0.12	0.13	47.9	1.5
Ta-3	1.13	7.90	0.24	0.08	0.09	32.0	2.2
Ta-4	0.85	5.93	0.18	0.06	0.06	24.0	3.0
Ta-5	0.68	4.74	0.14	0.05	0.05	19.2	3.7
Ta-6	0.57	3.95	0.12	0.04	0.04	16.0	4.5

(b) TTIP Concentration in the Reactant A[b]

Test No.	TTIP Concentration in the Reactant A [vol. %] C_{TTIP}
Tb-1	1.0
Tb-2	3.0
Tb-3	5.0
Tb-4	7.0
Tb-5	9.0

(c) H_2O Concentration in the Reactant B[c]

Test No.	H_2O Concentration in the Reactant B [vol. %] C_{water}
Tc-1	10.0
Tc-2	20.0
Tc-3	30.0
Tc-4	40.0
Tc-5	50.0

[a]$C_{TTIP} = 1.0$ vol. %, $C_{water} = 34.0$ vol. %, Temp = R.T. (=298 K).
[b]$Q_A = 3.40$ mL/min, $Q_B = 23.71$ mL/min, $C_{water} = 34.0$ vol. %, Temp = R.T. (=298 K).
[c]$Q_A = 3.40$ mL/min, $Q_B = 23.71$ mL/min, $C_{TTIP} = 1.0$ vol. %, Temp = R.T. (=298 K).

analysis of the mean size and distribution, and observe the shape of the fine particles.

Experimental Results and Discussion

Performance of titania fine particles formation on the concentric microreactor

We first performed an experiment to study the titania fine-particle formation performance of the concentric microreactor that we used. Figure 3a shows the size distribution of the fine particles formed in the microreactor under the experimental condition Ta-1, and that of the fine particles formed in a conventional-stirred vessel with the batch method under a sufficiently strong stirring condition. For the fine particle produced by microreactor, the median diameter $D_{P,50}$, was 47.5nm, coefficient of variation CV, was 24.23 %, which represents the spread of the particle-size distribution. Figure 3b is a SEM photograph of the fine particles formed in each experimental unit. It was shown that the size distribution of fine particles formed in the microreactor were narrower than those formed in the stirred vessel. Thus, it was characteristic that the particles formed in the microreactor tended to be smaller, as seen in the SEM photograph. This result shows a similar tendency to our findings (Takagi et al.[14]). This result of the median diameter agrees well with the one previously obtained under similar experiment conditions. We consider that such fine particles having narrow-size distribution were formed in the laminar flow for the following reason: The mixing of the reactants that would form titania fine particles occurred mainly due to the molecular diffusion via interface in the laminar flows of Reactants A and B, and, hence, the process of the nucleation and particle growth in the fine-particle formation was more ordered than that in the random mixing due to the turbulence-created vortices with the batch method. We can, therefore, expect from these characteristics that the multilamination type microreactor that utilized the molecular diffusion induced mixing process could realize accurate control of the particle size and distribution, which was difficult with the conventional-batch method.

In the case of a liquid-phase reaction by the molecular diffusion of two reactants, which are almost same molecular weight like this experiment, the diffusion rates of the reactants are almost same, so that the reaction would be conducted under the equivalent concentration condition. However, all reactions of fine-particle formation would not be like this type. For example, in the case of using two reactants which are quite different molecular weights, the diffusion rates are different in natural, and the reaction would proceed under undesired condition. In such a case, a proper diffusion state should be constructed so that both reactants encounter each other one by one. Now, we could design a multilamination structure with equivalent diffusion rates by changing lamination width, temperature or concentration profile.

Influence of the operation parameters

Figure 4 shows the experimental result of the median diameter and the coefficient of variation CV under various operational conditions. Figure 4a, b, and c, respectively, show the effects of the mean-residence time $T_{Ave.}$ in the microreactor, the TTIP concentration C_{TTIP} of Reactant A in Layer A, and the water concentration C_{Water} of Reactant B in Layer B.

From Figure 4a, it was shown that the median diameter increased with the mean-residence time $T_{Ave.}$. This may be because longer mean-residence time promotes molecular diffusion in the radial direction (r), perpendicular to the flow direction, of the annular pipe microchannel, and the nuclei formed near the reaction interface grow with the reactants supplied by the molecular diffusion. On the other hand, the CV is almost constant, independent of the increase of the mean-residence time T_{Ave} in this experiment. This fact indicates that, even

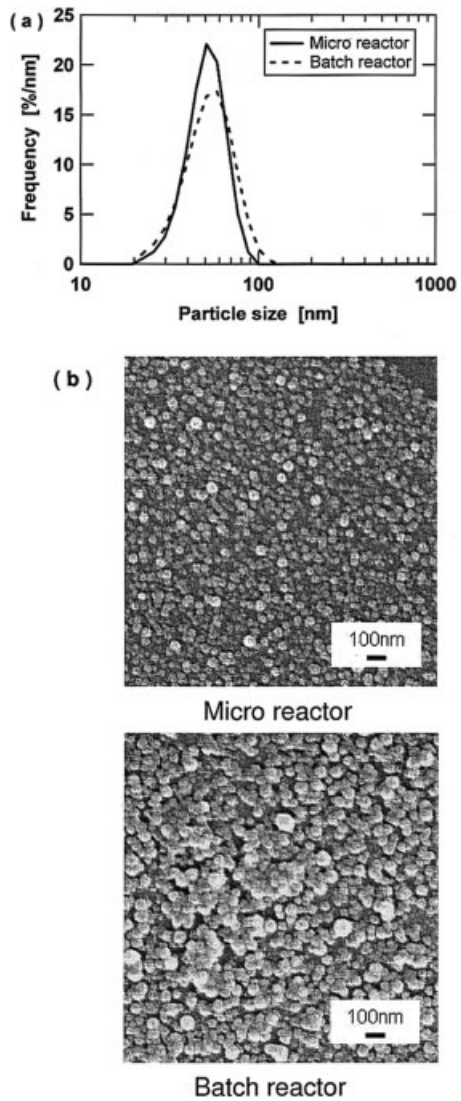

Figure 3. Comparison of the fine particles produced by the microreactor, and the batch reactor: (a) particle distributions, and (b) SEM photographs of fine particles.

when the mean-residence time is increased by decreasing the mean-linear velocities, the formed nuclei only grew as flowing in the downstream of the nucleation area of the microchannel without being newly formed nuclei during the particle-growth process (renucleation), vanishing, or aggregating.

Next we focus on the effect of each reactant concentration. In Figure 4b, the median diameter increased monotonically as the TTIP concentration increased. This occurred for the following reason. In the particle-growth process of the titania particle, the higher the TTIP concentration was, the larger the concentration gradient was, and, hence, the larger the diffusion rate of TTIP was from the central part of Layer A to the nuclei formed near the reaction interface in the upstream of the microchannel. This means that the amount of supplied TTIP per unit number of nuclei was large even when the mean-residence time was kept constant, and, therefore, nucleus growth was promoted. On the other hand, the CV was relatively small at a low TTIP concentration, and had superior monodispersibility, but in its overall behavior the CV was almost constant. This indicates that the nuclei were not newly formed during the particle growth (renucleation), vanished, or aggregated, but only grew when they flowed in the downstream of the nucleation area in the microchannel, even when the TTIP concentration increased in a certain range with the water concentration being kept at 34.0 vol. %, just like when we changed the mean-residence time. From Figure 4c, it was found that the CV were almost constant, but the median diameter was smallest when the water concentration is around 30 vol. %. When the water concentration was smaller than 30 vol. %, the supersaturation degree in the nucleation process became lower due to the insufficient water supply, and, hence, only a small number of nuclei are formed. In the particle-growth process of these nuclei, the low supply rate of water, and, hence, relatively high supply rate of

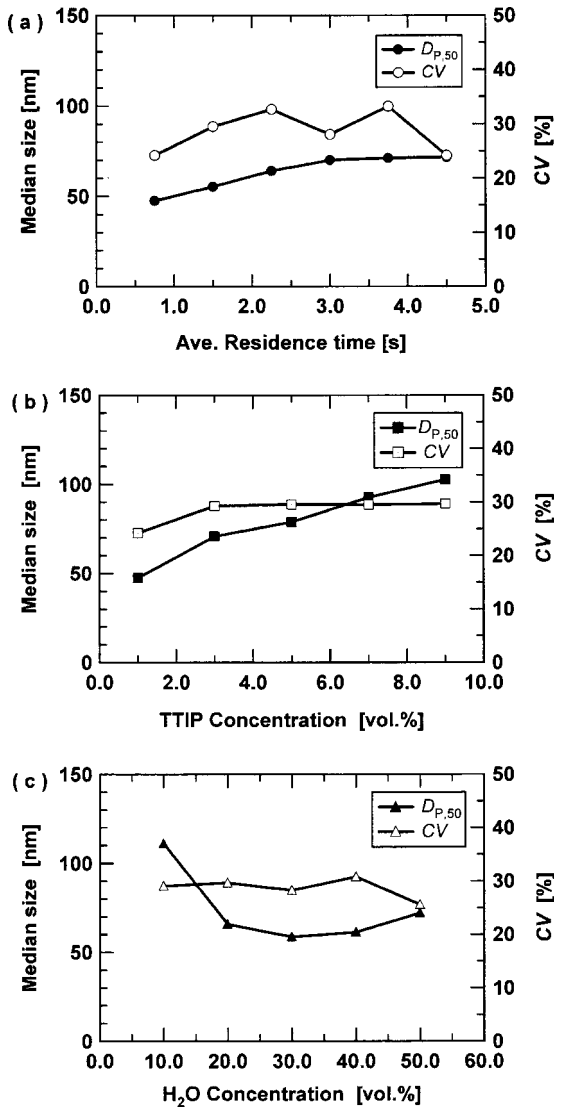

Figure 4. Influence of the operation parameters: (a) the average-residence time ($T_{Ave.}$), (b) the TTIP concentration (C_{TTIP}) in the Reactant A, and (c) the H_2O concentration (C_{Water}) in the Reactant B.

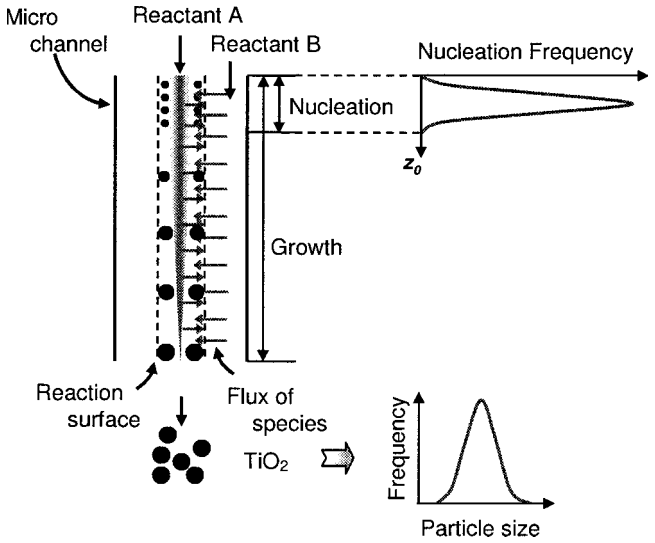

Figure 5. Presumed mechanism on titania fine-particle formation.

TTIP promoted nucleus growth, since the amount of the supplied TTIP per unit number of nuclei was large, as explained earlier regarding the effect of the TTIP concentration. On the other hand, when the water concentration was higher than 30 vol. %, the supersaturation degree in the nucleation process became higher due to the excessive water supply, and, hence, many small nuclei were formed. However, in the particle-growth process of these nuclei, excessively supplied water enhanced the dielectric constant around the nuclei, and developed an environment for the nuclei to aggregate, and the nucleus aggregation grows making the median diameter large.

Summarizing the earlier experimental results, we can presume the following mechanism of the titania fine-particle formation in the concentric microreactor, as illustrated in Figure 5 for easy understanding. At first, just after the merging point of the reaction solutions, namely at the reaction interface in the upstream of the microchannel, the movable, low-molecular-weight water in Layer B diffused into Layer A of the undiluted, highly concentrated TTIP, and increased the saturation degree over the minimum critical supersaturation, forming nuclei. The number of formed nuclei varied primarily with the diffusion rate of water, that is, the water concentration in Reactant B in Layer B. In higher-water concentration, many small size nuclei were formed. The reactants were supplied by the molecular diffusion, but largely consumed by the nucleation. As a result, the concentration of the reactants that stayed around the formed nuclei decreased, and the saturation degree became lower than the minimum critical supersaturation. At that point, the nucleation stopped. The formed nuclei flowed down in the microchannel without changing their positions in the radial direction of the channel, due to the stable laminar flow. The nuclei grew with the reactants, TTIP and water, being supplied from Layers A and B. In the TTIP concentration range and at the diffusion rate of TTIP in this experiment, renucleation or aggregation of nuclei did not occur in the downstream of the nucleation process area, and only the nucleus growth was promoted. On the other hand, at the diffusion rate of water in the experiment, the nucleus growth mechanism changed depending on whether the water concentration is over or below 30 vol. %. When the water concentration is below 30 vol. %, the formed nuclei seemed to grow monotonically, while when it is more than 30 vol. % the excessively supplied water enhanced the dielectric constant, and, hence, made the nuclei aggregate and grow.

Numerical Simulation

Based on the experimental results on the titania fine particle formation in the concentric microreactor, and on the mechanism of the fine-particle formation process derived from the analysis of the result, we proposed a relatively simple calculation model that realized the mechanism, and investigated its validity. We also examined a method to estimate nucleation region and the formation-frequency distribution from the model calculation result.

Fundamental equations

Since the microchannel in the concentric microreactor has a cylindrical shape with axial symmetry, we examined the flow in the microchannel in cylindrical coordinates (r, θ, z). Here, r is the coordinate in the radial direction of the microchannel, θ the coordinate in circumferential direction, and z the coordinate in the flow direction. The origin of the coordinates was set to the merging point of Reactants A and B, located on the concentric axis. The fundamental equations of dynamics are shown later. Here, we assumed that the fluids are single-phase incompressible Newtonian fluid with steady-laminar flow. According to the assumption of the laminar flow, we neglected the velocity in r direction (u_r), and in θ direction (u_θ). We also neglected gravitation. We omitted energy equations without any reference to the energy balance of temperature, reaction heat, and so on

Equation of continuity

$$\frac{\partial u_z}{\partial z} = 0 \tag{3}$$

Equation of motion

$$\rho u_z \frac{\partial u_z}{\partial z} = -\frac{\partial P}{\partial z} - \frac{1}{r}\frac{\partial}{\partial r}(r\tau_{rz})\tau_{rz} = -\mu\frac{\partial u_z}{\partial r} \tag{4}$$

Equation of diffusion

$$\frac{\partial C_A}{\partial z} = \frac{D_{AB}}{u}\left(\frac{\partial^2 C_A}{\partial r^2} + \frac{1}{r}\frac{\partial C_A}{\partial r}\right) \tag{5}$$

ρ : Fluid density [kg/m^3]; μ : Viscosity [mPa · s]

Simulation model

In the earlier fundamental equations the boundary condition is given by $C_1 = 0$ (since $\frac{\partial u_z}{\partial r} = 0$ at $r = 0$). Using the equation of continuity, equation of motion and boundary condition, we can derive the velocity-distribution equations in the dual-pipe microreactor, described by Eqs. 6–8. The volume flow rates of Reactants A and B are given by Eqs. 9 and 10. The pressure loss ΔP should be the same in the Eqs 9 and 10, and, hence, the interface location between the two fluids R_i can be expressed by Eq. 11.

Since $u_{z.in} = u_i$ at $r = R_i$, we have

$$u_{z.in} = \frac{\Delta P}{4L\mu_{in}}\left(R_i^2 - r^2\right) + u_i \ (0 \ \le \ r \ \le \ R_i) \tag{6}$$

Since $u_{z.out} = 0$ at $r = R_{out}$, we have

$$u_{z.out} = \frac{\Delta P}{4L\mu_{out}}\left(R_{out}^2 - r^2\right) \qquad (R_i \ \le \ r \ \le \ R_{out}) \tag{7}$$

Since $u_{z.out} = u_{z.in}$ at $r = R_i$, we have

$$u_i = \frac{\Delta P}{4L\mu_{out}}\left(R_{out}^2 - R_i^2\right) \tag{8}$$

$$Q_{in} = \int_0^{R_i} u_{z.in}\, 2\pi r dr = \pi u_i R_i^2 + \frac{\pi \Delta P}{8L\mu_{in}} R_i^4 \tag{9}$$

$$Q_{out} = \int_{R_i}^{R_{out}} u_{z.out}\, 2\pi r dr = \frac{\pi \Delta P}{8L\mu_{out}}\left(R_{out}^2 - R_i^2\right)^2 \tag{10}$$

$$R_i^2 = \frac{Q_{in}}{Q_{in}\mu_{out}} \frac{\left(R_{out}^2 - R_i^2\right)^2}{R_i^2\left(\frac{1}{\mu_{in}} - \frac{2}{\mu_{out}}\right) + \frac{2R_{out}^2}{\mu_{out}}} \tag{11}$$

ΔP is the pressure loss; subscript x_{in} is internal pipe fluid; subscript x_{out} is the annular area fluid, and subscript x_i is the interface between the two fluids.

On the other hand, the reactant-concentration distribution in the diffusion of TTIP and H_2O, was calculated by solving the earlier diffusion equation with the tridiagonal matrix analysis method (TDMA), an implicit method, by utilizing Microsoft Visual Basic (VBA).

We set the boundary conditions as follows.Initial and boundary conditions of TTIP

$$\begin{aligned}
&\text{I.C. at } z = 0, \quad C_A = C_0 \\
&\text{B.C. at } r = R_i, \quad C_A = 0 \qquad (0 \ \le \ z \ \le \ R_i) \\
&\text{B.C. at } r = 0, \quad \partial C_A/\partial r = 0 \quad (0 \ \le \ z \ \le \ R_i)
\end{aligned}$$

Initial and boundary conditions of H_2O

$$\begin{aligned}
&\text{I.C. at } z = 0, \quad C_A = C_0 \qquad (R_i \ \le \ z \ \le \ R_{out}) \\
&\text{I.C. at } z = 0, \quad C_A = 0 \qquad (0 \ \le \ z \ \le \ R_i) \\
&\text{B.C. at } r = 0, \quad \partial C_A/\partial r = 0 \quad (z > 0)
\end{aligned}$$

The diffusion constant D_{AB} was set to 1×10^{-9} m^2/s, and at $r = R_i$, we took account of the water solubility 26.28 mol. % in the octanol. From the calculation result, we obtained the TTIP consumption distribution in the microreactor, from which the reaction rate $X(z)$ was calculated by Eq. 12. Here F_{A0} presents the initial TTIP concentration, and $F_A(z)$ the retention concentration of TTIP at position z

$$X(z) = 1 - \frac{F_A(z)}{F_{A0}} \tag{12}$$

Next, we explain the formulation of the titania particle formation process model shown in Figure 5. The average particle size in the growing process can be derived from the mass balance Eq. (13) in the flow direction of the microreactor. Equations 12 and 13 give Eq. 14, from which we can calculate the mean particle size at the position z

$$V_{in}(C_{A0} - C_A(z)) = \frac{n\rho}{M}\frac{\pi}{6} D_P^3(z) \tag{13}$$

$$D_P(z) = \left(\frac{6MF_{A0}}{\pi n\rho} X(z)\right)^{1/3} \tag{14}$$

The symbols used in the equations are listed as: V_{in} as the volumetric flow rate in the internal pipe; m^3/s; C_{A0} is the initial concentration of TTIP, mol/m^3; F_{A0} is the molar flow rate of TTIP at the inlet of the microreactor, mol/s; n is the number of outflow particles from outlet of the microreactor per unit time, 1/s; ρ is the particle density, kg/m^3; 3820 kg/m^3 (Anatase-type particle density is assumed), and M is the molecular weight of titania, kg/mol; 7.988×10^{-3} kg/mol.

As for the boundary conditions, the mean-particle size $D_P(L)$, at the outlet of the microreactor ($z = L$) was set to the experimental data of the median diameter $D_{P,50}$, that were obtained in typical experimental conditions. From the boundary conditions we obtained the number of outflow particles per unit time, and modeled the distribution of the median diameter in the flow direction in the microreactor.

The nucleation area can be calculated from the experimental data of the particle-size distribution at the outlet of the microreactor ($z = L$). The calculation steps are shown later. Figure 6 illustrates the procedure.

1. By assuming that the largest particles in the size distribution obtained in the experiment were the ones that grew from the nuclei formed at the inlet of the microreactor, we calculate the number of particles with the particle-growth equation.

2. From the particle growth equation we calculate the growth of particles that are formed in the nucleation area. Figure 6a shows as an example the growth of the particles formed at $z =$ 0m (inlet of the microreactor), and $z = 0.04$ m. In the right of the figure, the vertical and horizontal axes of the size distribution are interchanged. In these figures the nucleation position, and the particle size at the outlet of the microreactor are linked to each other. That is, the particles formed at $z = 0$ m grow to the size $D_{P,MAX}$ at the outlet and those formed at $z = 0.04$ m to the size $D_{P,1}$.

3. From the result, we obtain Figure 6b, which shows the relation between the nucleation location and the particle size found at the outlet of the microreactor.

4. From Figure 6b and the particle-size distribution, we obtain Figure 6c, which presents the nucleation region and particle-formation frequency.

By following the earlier procedure, we can estimate the nucleation region and the frequency distribution.

Calculation Results and Discussion

Verification of simulation model

We first examined the validity of the velocity distribution in the microreactor obtained from Eqs. 6–8, by comparing it to that calculated with commercial numerical fluid dynamics software FLUENT 6.2, where we used the fluid-dynamics condition of the experimental condition Ta-1 in Table 1a. The veloc-

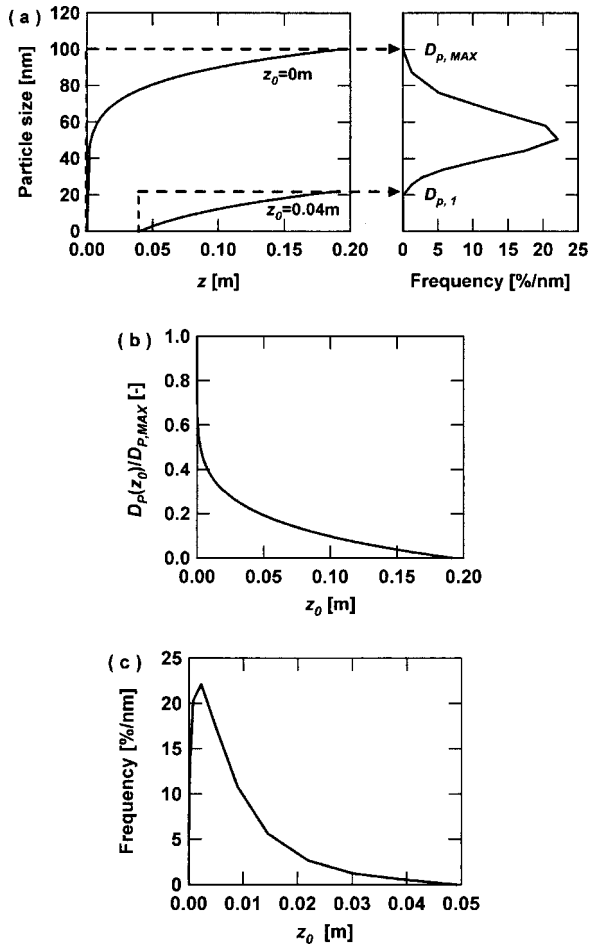

Figure 6. Calculation method for a nucleation region.

ity distribution at the outlet of the microreactor is shown in Figure 7. The calculation result derived from Eqs. 6–8 coincided with that obtained in FLUENT 6.2, which confirmed the validity of the model. It was also found that the interface between the two fluids sent from the internal and external pipes was located 198 μm from the central axis at the outlet, and there was small velocity gradient at that position. Therefore, we could presume that the reactants mixed not because of convection by shear caused from the velocity gradient, but just because of their diffusion.

Next we compared the calculated values of the median diameter in the model using Eqs. 5, 12, and 14 with the experimental data shown in Figure 4. The comparison result is given in Figure 8. Here we examined two parameters, the mean-residence time, $T_{\mathrm{Ave.}}$, and TTIP concentration C_{TTIP}. To study the effect of $T_{\mathrm{Ave.}}$, we calculated the median diameter at the outlet of the microreactor under each condition by assuming that the number of outflow particles per unit time was proportional to the mean-linear velocity $V_{\mathrm{Ave.}}$, based on the number of particles calculated from the median diameter that was obtained under the experimental condition Ta-3 of Table 1. As a consequence, the calculation result shows good agreement with the experimental result, as seen in Figure 8a. This indicates that the model is appropriate for demonstrating the influence of the mean linear velocity on the median diameter. On the other

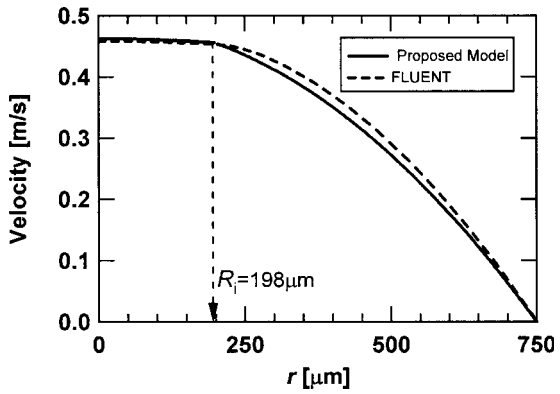

Figure 7. Calculation results on velocity profiles at the outlet of the microreactor between the proposed model and FLUENT 6.2., the commercial model.

hand, to study the effect of C_{TTIP}, we calculated the median diameter at the outlet of the microreactor under each condition by assuming that the number of outflow particles per unit time did not change with the TTIP concentration, based on the number of particles calculated from the median diameter that was obtained under the experimental condition Ta-1 of Table 1.

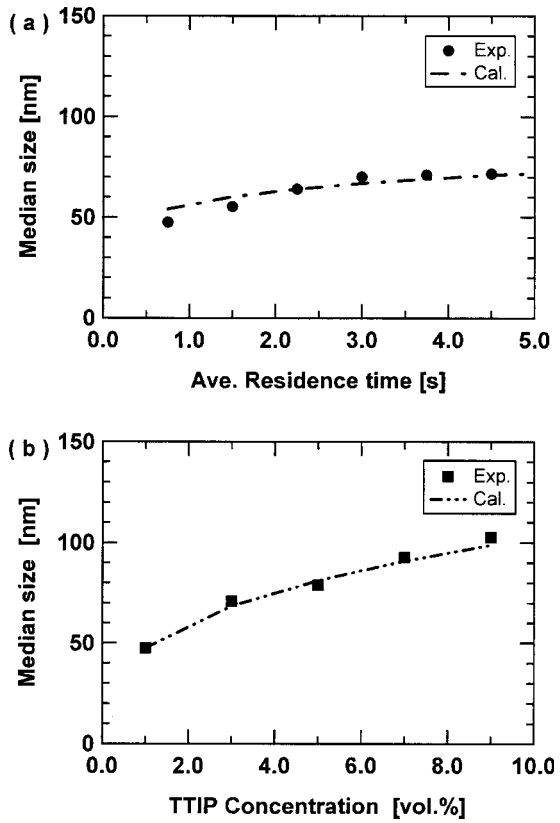

Figure 8. Simulation results of the median size compared with the experimental results: (a) the average-residence time ($T_{\mathrm{Ave.}}$), and (b) the TTIP concentration (C_{TTIP}) in the Reactant A.

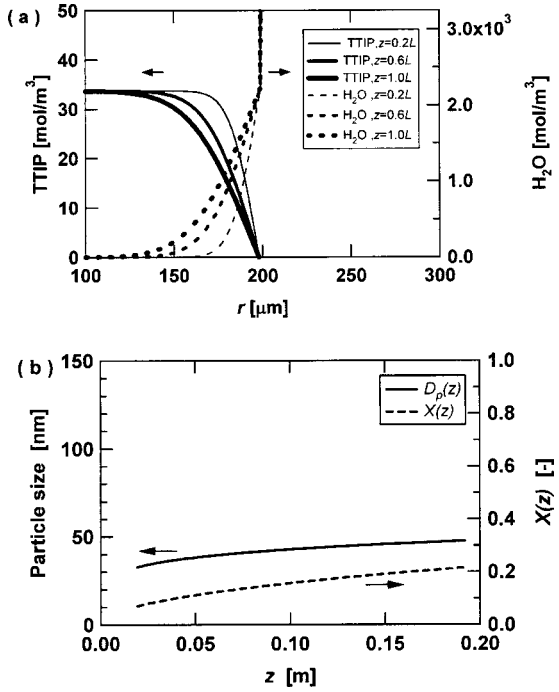

Figure 9. Change in the reactants-concentration profiles (a), and the median size with the flow direction length (b).

Then we found that the calculation result coincided well with the experimental result, as shown in Figure 8b, indicated that the model described the effect of the TTIP concentration appropriately. These two results verified clearly the validity of the model.

Discussion of mechanism on fine particle formation processes

In the earlier examinations, we discussed the estimation of particle sizes only at the outlet of the microreactor. Since the validity of the model has been presented, we now quantitatively analyze the behavior of the particle formation in the microreactor and discuss the particle-formation mechanism.

Figure 9 shows the calculation results obtained by utilizing experimental result under condition Ta-1 in Table 1. Figure 9a shows the concentration distributions of TTIP and H_2O in the flow direction in the microreactor. Figure 9b presents the behavior of the particle growth in the flow direction in the microreactor that we obtained from the TTIP reaction rate $X(z)$, which was calculated from the concentration distribution, and the median diameter at the outlet. Figure 9a clearly shows that the water diffused into the interface area (at $r = 198$ μm) between Reactants A and B, and the TTIP was consumed in the particle formation, making the concentration gradient smaller. We also found that the particle formation region at the outlet of the microreactor extended from the interface location $r = 198$ μm to the position around $r = 120$ μm. Figure 9b suggests that the reaction rate $X(L)$ at the outlet of the microreactor was about 0.2, and, hence, the nuclei formed in the vicinity of the merging point gradually grew in their growing process. It is, therefore, possible to estimate the reaction rate and growth rate of the particles at the outlet of the multilamination type microreactor that utilizes molecular diffusion to mix reaction solutions.

Figure 10 shows the model's estimation of the influence of the particle formation condition parameters, that is, the mean-linear velocity, $V_{\text{Ave.}}$, and the TTIP concentration C_{TTIP}, on the number of formed particles. Figure 10a indicates that the number of formed particles per unit time is proportional to $V_{\text{Ave.}}$ when the concentration of the supplied reaction solution (C_{TTIP}, C_{Water}) is constant. $V_{\text{Ave.}}$ corresponds to the volume of the reaction solution supplied in unit time to the microreactor, and, therefore, the particle-number density n is constant with no dependency on $V_{\text{Ave.}}$. Namely, when the concentration of the supplied reactant solutions (C_{TTIP}, C_{Water}) is constant, the nucleation finished and proceeded to the particle growth process as long as $V_{\text{Ave.}}$ stayed in the range of our experiment. We also found that the diffusion of the reactant in the reactant solution did not depend on the flow state at the mean-linear velocity, and could be treated as an independent event. Figure 10b shows that the number of the particles formed in unit time is constant with no dependency on C_{TTIP} if $V_{\text{Ave.}}$ of the supplied reactant solution is constant. C_{TTIP} is a parameter that affects the diffusion rate of the reactant TTIP to the reaction interface, the interface between Reactant A and Reactant B. Since this parameter did not affect the number of the nuclei formed in unit time, we can consider that the nucleation occurred instantaneously just after the merging point, independently of the TTIP concentration, and the diffusion rate had an influence

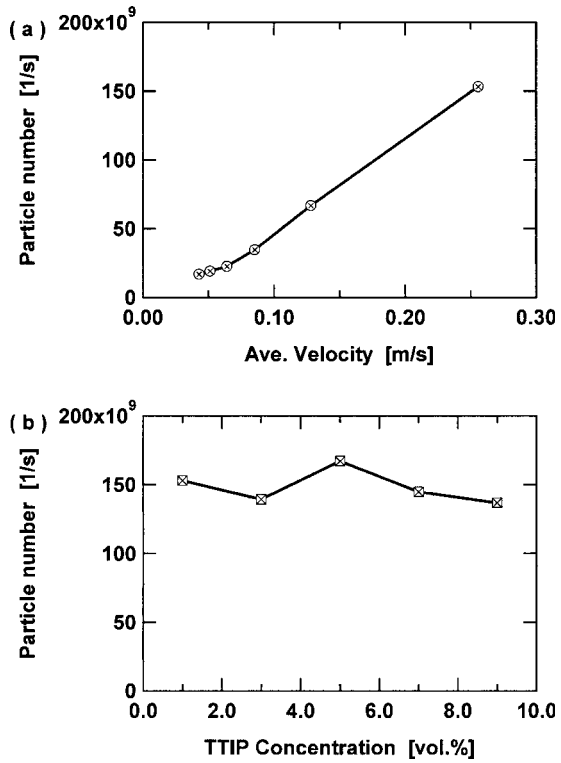

Figure 10. Predictions of the particle number with the operation conditions: (a) the average-residence time ($T_{\text{Ave.}}$), and (b) the TTIP concentration (C_{TTIP}) in the Reactant A.

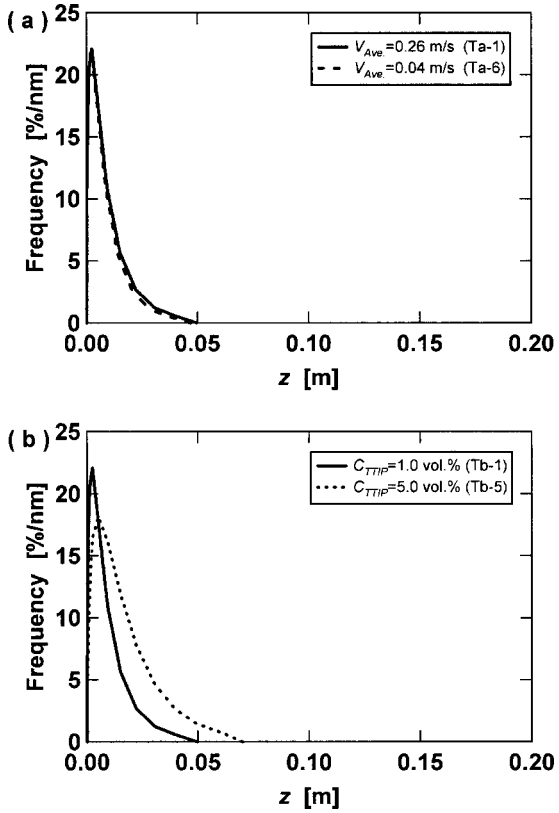

Figure 11. Predictions of the nucleation areas with the flow direction length: (a) the average-residence time ($T_{Ave.}$), and (b) the TTIP concentration (C_{TTIP}) in the Reactant A.

only on the nucleus growth. Our experiment indicated that, in the particle-growth process, there was no coalescence or aggregation of the particles and nuclei or the renucleation. This knowledge may indicate the controllability of the nucleation by changing the operation parameters, $V_{Ave.}$ and C_{TTIP}.

As indicated earlier, estimation of the nucleation behavior is important for the clarification of the fine-particle formation process. Here, we use the model to estimate the region and distribution of the nucleation. Figures 11a and b show the influence of the mean-linear velocity V_{Ave}, and the influence of the TTIP concentration C_{TTIP}, respectively. The figures suggest that, in every experimental condition, the nucleation starts suddenly after the reaction solutions merge and stops in about 0.05–0.07 m upstream in the microreactor. In terms of time, the nucleation finishes in several hundred milliseconds to about 1 s. The nucleation region does not vary with the mean-linear velocity, but extends to the downstream of the microchannel as C_{TTIP} becomes larger. This can be explained as follows. In the interface at the merging point where the two reaction solutions first encounter each other, the extremely large gradient in the concentration enhances the supersaturation rapidly, and a number of nuclei are formed. After that, the supersaturation near the interface, that is, the amount of formed nuclei, is determined by the balance between the amount of reactants consumed in the initial nucleation and the amount of reactants supplied by the molecular diffusion. However, with $V_{Ave.}$ in this experiment, the number of the initially formed nuclei dominated the later events, and the change of the supersaturation, caused by the aforementioned balancing, did not have a significant effect. When C_{TTIP} is large, the flux of the reactants supplied to the interface by the molecular diffusion is large, and it takes longer for the degree of saturation to become smaller than the minimum critical supersaturation. This is why the nucleation region extended to the downstream position of the microchannel. The reason why the number of particles was constant precipitate the long nucleation time is because the nucleus growth progressed simultaneously with the nucleation, and, hence, TTIP was consumed also in the particle-growth process, which resulted in the smaller number of the particles formed in unit time. Thus, the nucleation process can be controlled by changing the shape of the concentric microreactor, and the particle-formation-condition parameters.

Possibility of Nanoparticle Formation

Finally, we tried to form nanoparticles on the basis of the logic presented earlier. The trial was conducted by using low TTIP concentration solution (C_{TTIP} = 0.05 vol. %), and the other conditions were same as the test conditions of Tb-1. Figure 12 shows the size distribution and TEM photograph of the particles produced. The $D_{P,50}$ and CV were 3.1 nm and 15.0 %, respectively, and the nanoparticles with narrow distribution were formed. This suggests that the particle growth was suppressed by reducing the diffusion rate of TTIP after the sharp nucleation in a small reaction zone under the low TTIP concentration. Thus, it was shown that fine particles could be produced precisely in the range of nanometer to submicronmeter orders by utilizing the proposed concentric microreactor.

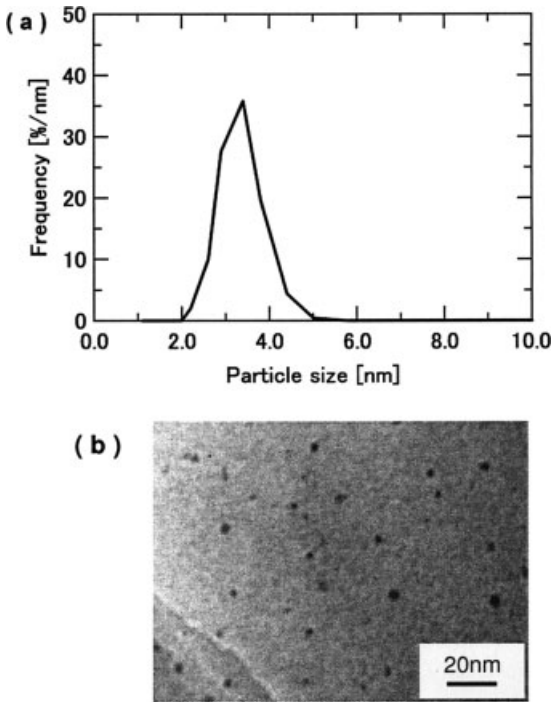

Figure 12. Particle-size distribution and the TEM photograph of titania produced under low TTIP concentration.

Conclusions

We conducted a titania fine-particle formation experiment using a concentric microreactor. The titania fine particles obtained in the microreactor exhibited small and narrow-size distribution, as compared with those obtained in a conventional-batch reactor. We also investigated the relation between the control-condition parameters of the microreactor (mean-residence time $T_{Ave.}$, TTIP concentration C_{TTIP}, and H_2O concentration C_{Water}), and the size and distribution of the titania fine particles. We clarified that, as $T_{Ave.}$ or C_{TTIP} increased, the median diameter increased with the coefficient of variation CV being kept constant. Next, we made a hypothesis on the titania fine-particle formation mechanism, based on the analysis of the experimental results, and developed a relatively simple calculation model. In the comparison of the calculated values from the model and the experimental values, we found good agreement, and, hence, confirmed the validity of the hypothetical mechanism of the titania fine-particle formation and the calculation model. We also used the model to calculate the reactant-concentration distribution, particle-growth rate, number of formed particles, and nucleation region, and analyzed the fine-particle formation process in detail. Consequently, it was found that the number of formed particles per unit volume was constant, and did not depend on the volume flow rate when the concentration of the supplied reaction solution was constant. Nucleation occurred immediately after the reaction solution merged and completed in the upstream of the microchannel. It was also found that the nucleation region extended toward the downstream as the TTIP concentration increases, regardless of the mean linear velocity of the reaction solution. Thus we established a technique to estimate the nucleation region, which is an important factor in particle formation, the particle-formation-frequency distribution in the region, and the behavior of the particle growing process. Finally, we tried to form nanoparticles less than 10 nm, on the basis of the earlier logic, and we successfully produced the nanoparticles of 3 nm with a narrow distribution under the low TTIP concentration. The study on the titania-fine particles shown here provides a guideline for designing microreactors to form other kinds of fine particles and yields industrially valuable information.

Acknowledgments

The research was conducted with the aid of The Research Association of Micro Chemical Process Technology (MCPT), for the project of Micro-Chemical Technology for Production, Analysis, and Measurement Systems, financially supported by New Energy and industrial Development Organization (NEDO). We acknowledge to MCPT and NEDO for their assistance. We also thank Mr. Takayuki Fujiwara (FUJIFILM Corp.) for fabricating the concentric microreactor.

Literature Cited

1. Matsumura Y, Maeda H. A new concept for macromolecular therapeutics in cancer chemotherapy: mechanism of tumoritropic accumulation of proteins and the antitumor agent smancs. *Cancer Res*. 1986;46:6387–6392.
2. LaMer VK, Dinegar HR. Theory, Production and Mechanism of Formation of Monodispersed Hydrosols. *J Am Chem Soc*. 1950;72:4847–4854.
3. Sugimoto T. Monodispersed Particles. New York; Elsevier; 2001.
4. Park HK, Kim DK, Kim CH. Effect of Solvent on Titania particle formation and morphology in thermal hydrolysis of $TiCl_4$. *J Am Ceram Soc*. 1997;80:743–749.
5. Ogihara T, Mizutani N, Kato M. Growth mechanism of monodispersed ZrO_2 particles. *J Am Ceram Soc*. 1989;72:421–426.
6. Kim KD, Bae HJ, Kim HT. Synthesis and growth mechanism of TiO_2 -coated SiO_2 fine particles. *Colloids and Surfaces A*. 2003;221:163–173.
7. Schenk R, Hessel V, Werner B, Schönfeld F, Hofmann C, Donnet M, Jongen N. Micromixers as a tool for powder production. *Chem Eng Trans*. 2002;1:909–914.
8. Nakamura H, Yamaguchi Y, Miyazaki M, Maeda H, Uehara M, Mulvaney P. Preparation of CdSe nanocrystals in a micro-flow-reactor. *Chem Commun*. 2002;23:2844–2845.
9. Wang H, Li X, Uehara M, Yamaguchi Y, Nakamura H, Miyazaki M, Shimizu H, Maeda H. Continuous synthesis of CdSe-ZnS composite nanoparticles in microfluidic reactor. *Chem Commun*. 2004;1:48–49.
10. Mae K, Maki T, Hasegawa I, Eto U, Mizutani Y, Honda N. Development of a new micromixer based on split/recombination for mass production and its application to soap free emulsifier. *Chem Eng J*. 2004;101:31–38.
11. Wille Ch, Gabski, H-P, Haller Th, Kim H, Unverdorben L, Winter R. Synthesis of pigments in a three-stage microreactor pilot plant -an experimental technical report. *Chem Eng. J*. 2004;101:179–185.
12. Wagner J, Kirner T, Mayer G, Albert J, Köhler MJ. Generation of metal nanoparticles in a microchannel reactor. *Chem Eng J*. 2004;101:251–260.
13. Schenk R, Hessel V, Jongen N, Buscaglia V, Guillemet-Fritsch S, Jones A. Nanopowders Produced Using Microreactors. In: Nalwa HS, ed-in-chief. Encyclopedia of Nanoscience and Nanotechnology. Vol 7. Stevenson Ranch, CA: American Scientific Publishers; 2004:287–296.
14. Hessel V, Löwe H, Schönfeld F. Micromixers - a review on passive and active mixing principles. *Chem Eng Sci*. 2005;60:2479–2501.
15. Nagasawa H, Aoki N, Mae K. Design of a new micromixer for instant mixing based on the collision of micro segments. *Chem Eng Technol*. 2005;28:324–330.
16. Schwarzer H-C, Peukert W. Experimental investigation into the influence of mixing on nanoparticle precipitation. *Chem Eng Technol*. 2002;25:657–661.
17. Schwarzer H-C, Peukert W. Tailoring particle size through nanoparticle precipitation. *Chem Eng Comm*. 2004;191:580–606.
18. Schwarzer H-C, Peukert W. Combined experimental/numerical study on the precipitation of nanoparticles. *AIChE J*. 2004;50:3234–3247.
19. Schwarzer H-C, Schwertfirm F, Manhart M, Schmid H-J, Peukert W. Predictive simulation of nano particle precipitation based on the population balance equation. *Chem Eng Sci*. 2006;61:167–181.
20. Wille Ch, Autze V, Kim H, Nickel U, Oberbeck S, Schwalbe Th, Unverdorben L. Progress in Transferring Microreactors from Lab into Production an Example in the Field of Pigments Technology. Proceedings of the 6th International Conference on Microreaction Technology. New Orleans, LA. 2002:7–17.
21. Takagi M, Maki T, Miyahara M, Mae K. Production of titania nanoparticles by using a new microreactor assembled with same axle dual pipe. *Chem Eng J*. 2004;101:269–276.

Manuscript received July 19, 2006, and revision received Oct. 9, 2006.